The Detection and Importance of Subtle Biofacies within a Single Lithofacies: The Upper Ordovician Kope Formation of the Cincinnati, Ohio Region

STEVEN M. HOLLAND
Department of Geology, University of Georgia, Athens, GA 30602-2501

ARNOLD I. MILLER and DAVID L. MEYER
Department of Geology, University of Cincinnati, Cincinnati, OH 45221-0013

BENJAMIN F. DATTILO
Department of Geosciences, Weber State University, Ogden, UT 84408

PALAIOS, 2001, V. 16, p. 205–217

Environmental controls on the distribution of fossils most commonly are found by recognizing that certain distinctive fossil assemblages are associated with particular lithofacies. Lack of change in lithofacies commonly is used as indicating a lack of significant environmental effects on the stratigraphic distribution of fossils. The results presented here challenge that view. The Upper Ordovician Kope Formation of the Cincinnati, Ohio, area has long been considered a single unit, both lithostratigraphically and in terms of depositional environment. Gradient analysis of over 1000 fossil assemblages reveals subtle environmental control on the distribution of fossils, in the absence of obvious lithologic change. This gradient analysis is used to construct an ecological model of the Kope fauna, with values of preferred depth, depth tolerance, and peak abundance estimated for the most common fossils. This method, conducted within a single lithofacies, offers the potential for reconstructing sequence architecture because faunas can be more sensitive recorders of environment than lithofacies. In addition, the presence of subtle facies control as in the Kope raises the prospect that environmental controls on paleobiologic and biostratigraphic patterns may be more pervasive than generally acknowledged.

INTRODUCTION

Paleontologists have long recognized environmental control on the distribution of fossils. However, most reports of environmental controls have come from cases in which lithofacies obviously differ from one another, making the recognition of facies control on fossils straightforward (e.g., Bayer and McGhee, 1985; Patzkowsky, 1995). This approach has led elsewhere to suggestions that the absence of changing lithofacies is evidence of a lack of environmentally controlled fossil distributions. For example, evolutionary studies are preferred where facies are unchanging, presumably because environmental conditions were relatively stable and, therefore, fossil faunas are not influenced by changes in environment (e.g., Sheldon, 1996). Although several researchers have recognized that fossils are more sensitive to environmental changes than are lithofacies (e.g., Springer and Bambach, 1985; Miller, 1988, 1997; Brett, 1998), empirical support for this argument has been limited.

The Upper Ordovician Kope Formation of the Cincinnati, Ohio, region exemplifies this problem well. Although workers in the late 1800s and early 1900s recognized faunal variations within the Kope (summarized in Caster et al., 1955), modern workers have tended to overlook them (but see Anstey and Perry, 1973; Anstey et al., 1987; Anstey and Rabbio, 1990). Upon broad inspection, the Kope gives the impression that it contains a single suite of fossil taxa that vary unsystematically in their relative abundance. Here, Kope faunas are shown to be far more structured than previously recognized, and this variation is interpreted to be environmentally driven. Strong evidence exists that the composition of faunal collections from the Kope changes with inferred water depth. The lack of obvious lithofacies change in the Kope suggests that depth control on faunas may be more common than currently recognized. The existence of such widespread depth control has significance for stratigraphic patterns of fossil occurrences, in general, and for the application of confidence limits to fossil ranges.

BACKGROUND

The 65-m-thick Kope Formation, and the rest of the type Cincinnatian Series, are interpreted to have been deposited on a northward-dipping, storm-dominated, mixed carbonate-siliciclastic ramp (Tobin, 1982; Holland, 1993; Jennette and Pryor, 1993; Brett and Algeo, 1999a). Although the dip of the ramp may have had a slight eastward or westward component, the generally northward dip throughout the Late Ordovician is shown by the consistent occurrence of shallower water facies in Kentucky and deeper water facies in Ohio and Indiana (Weir et al., 1984; Holland, 1993). The north-south alignment of gutter casts and the east-west orientation of megaripple crests within the Kope also are consistent with an east-west strike to the ramp (Duke, 1990; Jennette and Pryor, 1993).

The Kope consists mostly of siliciclastic mudstone (60–94%, median 80%), followed by varying amounts of calcisiltite (0–16%, median 4%), skeletal packstone and grainstone (0–35%, median 14%), with much smaller proportions of lime mudstone and wackestone. Calcisiltite beds display a wide array of sedimentary structures including small-scale hummocky and trough cross-lamination, planar lamination, vortex ripples, current ripples, gutter casts, prod marks, *Kinneyia* and millimeter ripples (Jennette and Pryor, 1993; Brett and Algeo, 1999a). Beds of skeletal packstone and grainstone commonly have erosional bases, and may display megaripples and large-scale cross stratification (e.g., sets thicker than 5 cm). Siliciclastic mudstones are graded into 3–5 cm event beds, with slightly silty bases. Collectively, these features are interpreted as storm beds (Kreisa et al., 1981; Tobin, 1982; Jennette and Pryor, 1993; Holland et al., 1997; Brett and Algeo, 1999a). The Kope has been interpreted as an offshore facies affected only by the strongest storms (Hay, 1981; Tobin, 1982; Holland, 1993; Jennette and Pryor, 1993; Brett and Algeo, 1999b).

Several workers have recognized lithologic cyclicity in the Kope (Hay, 1981; Tobin, 1982; Jennette and Pryor, 1993; Holland et al., 1997; Brett and Algeo, 1999a). Meter-scale cycles in the Kope consist of alternations of mudstone-rich intervals and limestone-rich intervals, although individual descriptions and interpretations of this cyclicity vary widely (see discussions in Holland et al., 1997, 1999). It remains unclear whether these alternations reflect cyclic changes in water depth or variations in storm frequency and intensity. Furthermore, some have questioned the existence of these meter-scale cycles by arguing that the pattern of lithologic change cannot be distinguished from randomness (Wilkinson et al., 1997).

Kope meter-scale cycles are bundled into larger-scale 20-m cycles in which the meter-scale cycles are initially thicker than average, but upsection become average to thinner than average. The origin of these 20-m cycles is also uncertain, although the organization of their component meter-scale cycles, coupled with clear stacking patterns of limestone-rich and mudstone-rich intervals in the subsurface (Dattilo, 1996) suggest that they are the result of relative fluctuations in sea level (Jennette and Pryor, 1993; Holland et al., 1997). The organization and delineation of these 20-m cycles is not entirely unambiguous, and different workers have developed somewhat different characterizations. All of these disagreements over the structure, origin, and even the presence of both scales of cyclicity within the Kope underscore that these cyclic lithologic variations are subtle.

Although the Kope contains a spectrum of lithologies, their interbedding within the Kope is repetitive and the Kope displays only weak large-scale changes in the relative proportions of these lithologies. This persistent fine-scale interbedding of lithologies has frustrated most attempts to subdivide the Kope into smaller lithostratigraphic or lithofacies units (but see Brett and Algeo, 1999c). As a result, the Kope is considered to be a single lithostratigraphic unit (Weiss and Sweet, 1964; Weir et al., 1984; Tobin, 1986). For the same reasons, the Kope has been regarded as either a single lithofacies or as two or three intimately and repetitively interbedded lithofacies (Hay, 1981; Tobin, 1982; Weir et al., 1984; Holland, 1993; Jennette and Pryor, 1993). To see firsthand the difficulty of subdividing the Kope into member-scale lithostratigraphic units, the measured sections in Jennette and Pryor (1993) and Holland et al. (1997) should be examined.

Compared to the strata, Kope faunas have received much less attention. Most studies have either treated the Kope collectively (e.g., Lorenz, 1973; Harrison and Mahan, 1981; Holland, 1993) or have focused on particular elements, such as bryozoans (Anstey and Perry, 1973) or hardground faunas (Wilson, 1985). None of these have examined systematically the stratigraphic changes of the entire Kope fauna in detail.

The fauna of the Kope is diverse and abundant. Although Dalvé (1948) lists 240 species from the Kope, few of these are common (Table 1). Epifaunal suspension feeders, such as brachiopods, bryozoans, and crinoids, are dominant. Trilobites are also locally common, as are bivalves, gastropods, cephalopods, ostracods, and graptolites.

METHODS

As part of a larger project on high-resolution correlation within the Kope Formation, five outcrops were measured in detail (Fig. 1). All but the lowest 10 m of the Kope is exposed at the K445 section, and all of the Kope is exposed at Holst Creek, although poorly so through most of the middle interval. Only portions of the Kope are exposed at Miamitown, Aurora, and Hume. At each locality, the exposed Kope Formation was measured, with the lithology, sedimentary structures, and fauna of every bed thicker than 0.5 cm recorded. The details of the lithologic descriptions and their results have been published previously (Holland et al., 1997, 1999, 2000; Miller et al., 1997).

To describe the fauna, every fossiliferous horizon was excavated, washed in the field, and the relative abundance of each taxon tallied. Beds of skeletal packstone and grainstone, and the soles of calcisiltite beds produced most of the fossils, although some mudstones were fossiliferous and included in this study. Relative abundance was scored as rare (1–2 specimens per 1000 cm^2), common (3–10 specimens per 1000 cm^2), or abundant (>10 specimens per 1000 cm^2). Most taxa were identified to genus wherever possible, including brachiopods, crinoids, trilobites, bivalves, cephalopods, and gastropods. Most bryozoans were classified on zooarial morphology, including thin bifoliate (<5 mm), thick bifoliate (>5 mm), thin ramose (<5 mm), thick ramose (>5 mm), and encrusting forms. Cryptostome and fenestellid bryozoans were listed as such, and the distinctive bryozoans *Escharopora, Aspidopora, Prasopora, Stomatopora* and *Parvohallopora* were described to the genus level.

These field descriptions resulted in a relative abundance matrix consisting of 1949 samples and 57 taxa. To minimize the effects of extremely rare taxa, all taxa occurring in only one sample were removed. Likewise, samples containing only a single taxon were removed. This culling resulted in a final matrix of 1337 samples and 46 taxa.

This matrix was analyzed with Detrended Correspondence Analysis, also known as DCA or Decorana (Hill and Gauch, 1980; McCune and Mefford, 1997). DCA is a multivariate statistical technique widely used with ecological data to ordinate taxa along underlying ecological gradients. Although other techniques, such as Correspondence Analysis, Principal Components Analysis, and Polar Or-

TABLE 1—Kope taxa analyzed in this study.

Low Epifaunal Suspension Feeders	High Epifaunal Suspension Feeders	Epifaunal Scavengers, Grazers, and Deposit Feeders	Carnivores & Parasites	Other
Bryozoans Encrusters *Escharopora* Fenestellids *Aspidopora* *Stomatopora*	**Bryozoans** Cryptostomes *Parvohallopora* Thick bifoliate Thick ramose Thin bifoliate Thin ramose	**Univalved Molluscs** *Cyclora* Unidentified gastropods (includes monoplacophorans)	**Gastropoda** *Cyclonema* **Hydrozoans** **Annelida** Scolecodonts	Graptolites (Planktonic suspension feeders) *Pseudolingula* (Infaunal suspension feeding inarticulates)
Inarticulates *Craniops* *Schizocrania* **Articulates** *Dalmanella* *Platystrophia* *Plectorthis* *Prasopora* *Rafinesquina* *Sowerbyella* *Strophomena* *Zygospira* **Annelida** *Cornulites* **Bivalvia** *Ambonychia* *Modiolopsis*	**Crinoidea** *Cincinnaticrinus* *Ectenocrinus* *Iocrinus* *Merocrinus* *Glyptocrinus*	**Trilobita** *Ceraurus* *Cryptolithus* Calymenids (includes *Flexicalymene* and *Gravicalymene)* *Isotelus* *Acidaspis* *Proetidella*	**Cephalopods** (includes primarily *Treptoceras*, but also *Ordogeisonoceras* and endocerids)	*Lepidocoleus* (Machaeridians of uncertain life habits) Nuculoids (Infaunal deposit feeding bivalves) Ostracods (nekto-benthic scavengers)

dination, also can be used to ordinate ecological data, they tend to distort the data such that the principal gradient underlying the data no longer corresponds directly to axis 1 (Minchin, 1987). Instead, this principal gradient is distributed among axes 1 and 2, producing what is known as the arch effect for Correspondence Analysis and the horseshoe effect for Principal Components Analysis. This arch is produced primarily when samples from the extremes of axis 1 contain such different assemblages that there is little overlap in their taxonomic composition. DCA flattens the Correspondence Analysis arch by dividing the arch into a series of segments and subtracting the mean axis 2 value for each segment from each score within that segment. This procedure has the side effect of tending to compress faunal variation near the ends of axis 1. This unwanted compression is then removed by rescaling axis 1 scores such that there is a constant rate of turnover along axis 1. The end result is that axis 1 reflects the primary source of ecological variation in the composition of faunas (for a more detailed explanation, see Hill and Gauch, 1980). Axes 2 and 3 reflect additional sources of variation beyond the principal gradient, but their interpretation is often much less clear because DCA is known to take variation that should be expressed on axis 2 and express some of it on axis 3 (Kenkel and Orlóci, 1986; Minchin, 1987).

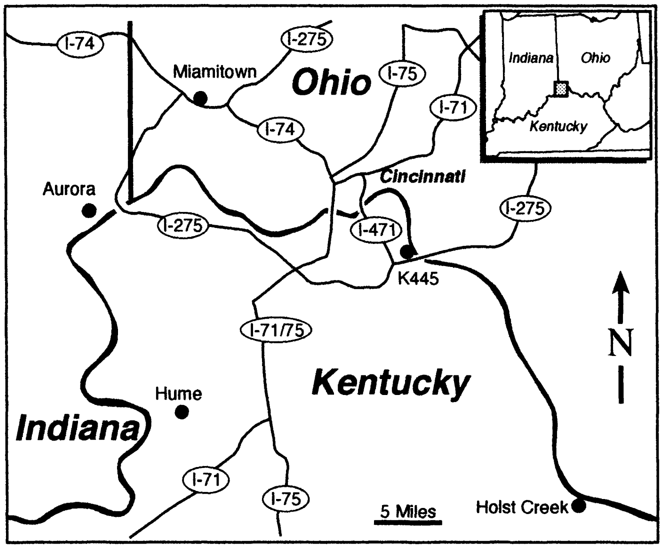

FIGURE 1—Map of study area, showing the locations of the five measured and sampled outcrops.

PC-ORD, Version 3.0 (McCune and Mefford, 1997) was used to run DCA because of its simplicity of data entry, culling, analysis, and plotting, as well as its ability to handle large data sets. Default settings were used for rescaling axes (on), rescaling threshold (0), and number of segments (26). The downweighting of rare taxa option was used to further minimize the distortions they cause. This option downweights in proportion to their abundance any taxa rarer than Fmax/5, where Fmax is the frequency of the most common taxon. Taxa more abundant than Fmax/5 are unaffected. Although only one of the DCA runs is reported here, several others were performed using different suites of samples or taxa, not using the rare taxon downweighting option, and using a percent transform on the data. All of these produced very similar results, indicating the robustness of the underlying structure in the data.

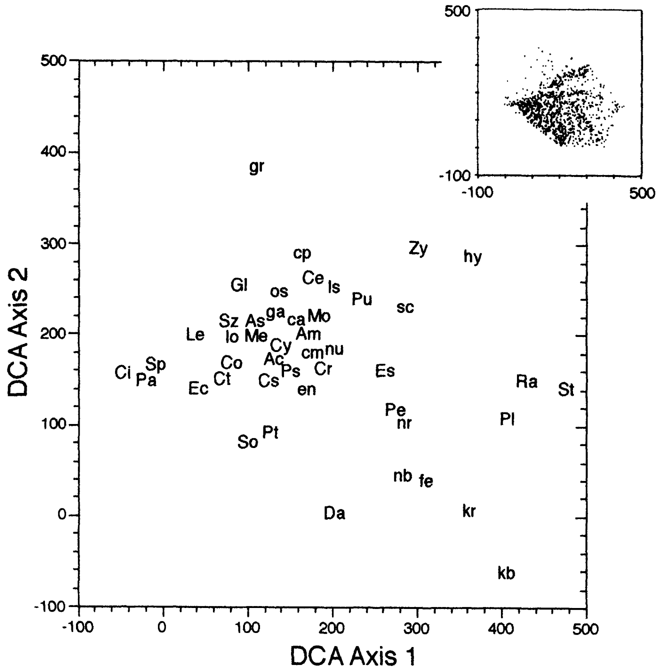

FIGURE 2—Axis 1 and axis 2 taxon scores (n = 46) from detrended correspondence analysis (DCA), with inset of sample scores (n = 1337) in upper right. Axis 1 is interpreted to reflect water depths, with low scores corresponding to deeper water and high scores corresponding to shallower water. Axis 2 may reflects a gradient in life habit, with low scores dominated by epifaunal suspension feeding taxa and high scores dominated by infaunal to semi-infaunal deposit and suspension feeders, as well as planktonic and nektonic forms. Ac: *Acidaspis*. Am: *Ambonychia*. As: *Aspidopora*. ca: calymenids. Ce: *Ceraurus*. Ci: *Cincinnaticrinus*. cm: cryptostomes. Co: *Cornulites*. cp: cephalopods. Cr: *Cyclora*. Cs: *Craniops*. Ct: *Cryptolithus*. Cy: *Cyclonema*. Da: *Dalmanella*. Ec: *Ectenocrinus*. en: encrusting bryozoans. Es: *Escharopora*. fe: fenestellids. ga: gastropods. Gl: *Glyptocrinus*. gr: graptolites. hy: hydrozoans. Io: *Iocrinus*. Is: *Isotelus*. kb: thick bifoliate bryozoans. kr: thick ramose bryozoans. Le: *Lepidocoleus*. Me: *Merocrinus*. Mo: *Modiolopsis*. nb: thin bifoliate bryozoans. nr: thin ramose bryozoans. nu: nuculoids. os: ostracods. Pa: *Parvohallopora*. Pe: *Plectorthis*. Pl: *Platystrophia*. Ps: *Prasopora*. Pt: *Proetidella*. Pu: *Pseudolingula*. Ra: *Rafinesquina*. sc: scolecodonts. So: *Sowerbyella*. Sp: *Stomatopora*. St: *Strophomena*. Sz: *Schizocrania*. Zy: *Zygospira*.

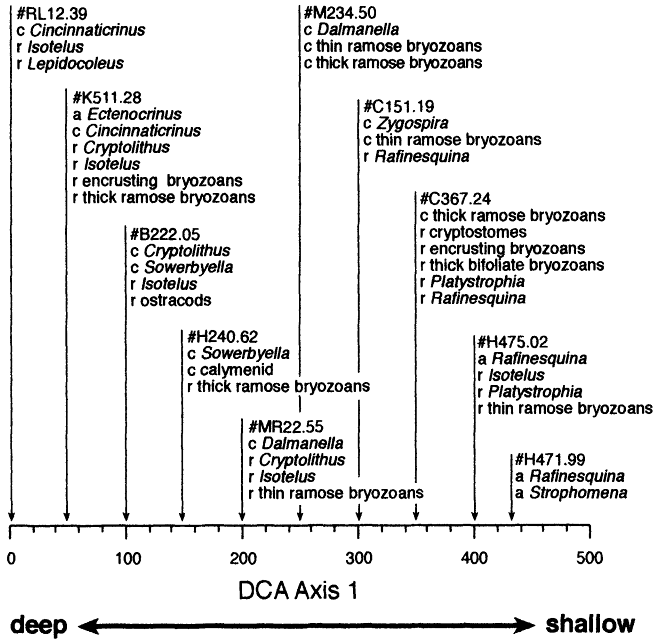

FIGURE 3—Typical sample compositions from selected points along axis 1. Relative abundance coded as a (abundant), c (common), and r (rare); see text for explanation of these classes.

DCA RESULTS

Biofacies

DCA simultaneously calculates Kope taxon scores and sample scores, and plots them on the same axes with the same scales (Fig. 2). Kope faunas vary continuously across axis 1 without evidence of abrupt breaks in faunal composition. Nonetheless, it is possible to examine the composition of representative samples along this axis (Figs. 3, 4). At extremely low values (0–50) on axis 1, assemblages are dominated by the crinoids *Cincinnaticrinus* (Fig. 4A) and *Ectenocrinus* (Fig. 4B), and may contain a variety of other taxa in much lower abundance, such as trilobites, machaeridians, ostracods, and cornulitids. At somewhat higher values (100–150), an assemblage consisting of the brachiopod *Sowerbyella* and the trilobite *Cryptolithus* occurs (Fig. 4C, D). The *Sowerbyella-Cryptolithus* assemblage also commonly has a wide variety of other taxa encountered in lower abundance. At higher axis 1 values (200–250), the *Sowerbyella-Cryptolithus* assemblage gives way to an assemblage dominated by the brachiopod *Dalmanella* (Fig. 4F). The trilobites, *Flexicalymene* and *Gravicalymene,* as well as the trilobite *Isotelus,* and bryozoans (chiefly encrusting, thin ramose and thin bifoliate forms) all commonly occur in the *Dalmanella* association. At axis 1 values of 300–350, *Dalmanella* gives way to the brachiopod *Zygospira,* a diverse association of bryozoans, and a small form of the brachiopod *Platystrophia* (Fig. 4G). At the highest observed values (400–430), assemblages are dominated overwhelmingly by the brachiopods *Rafinesquina* and *Strophomena* (Fig. 4H). Based on several lines of evidence (see below), Axis 1 is interpreted to reflect water depth.

Previous analyses and replicate analyses described above indicate that this underlying structure is robust. In a cluster analysis of the uppermost 8 meters of the Kope, as well as the overlying Fairview and Bellevue Formation, Diekmeyer (1998) found comparable assemblages, including an *Onniella* (= *Dalmanella*)-crinoid-trilobite, *Onniella*-bryozoan, *Zygospira*-graptolite-trilobite, *Zygospira*-

→

FIGURE 4—Photographs of slabs illustrating common assemblages, generally ordered along DCA axis 1, from lowest on axis 1 (A) to highest (H). Scale bar in each photo represents 1 cm. A: *Cincinnaticrinus* (Ci). B: *Ectenocrinus* (Ec). C: *Sowerbyella* (So), *Cincinnaticrinus* (Ci), and *Dalmanella* (Da). D: calymenid (ca), thin ramose bryozoans (nr), thin bifoliate bryozoans (nb), *Cryptolithus* (Ct), and *Acidaspis* (Ac). E: gastropods (ga) and thick ramose bryozoans (kr). F: *Dalmanella* (Da) and *Glyptocrinus* (Gl). G: *Dalmanella* (Da), thick ramose (kr) and thick bifoliate (kb) bryozoans. H: *Rafinesquina* (Ra).

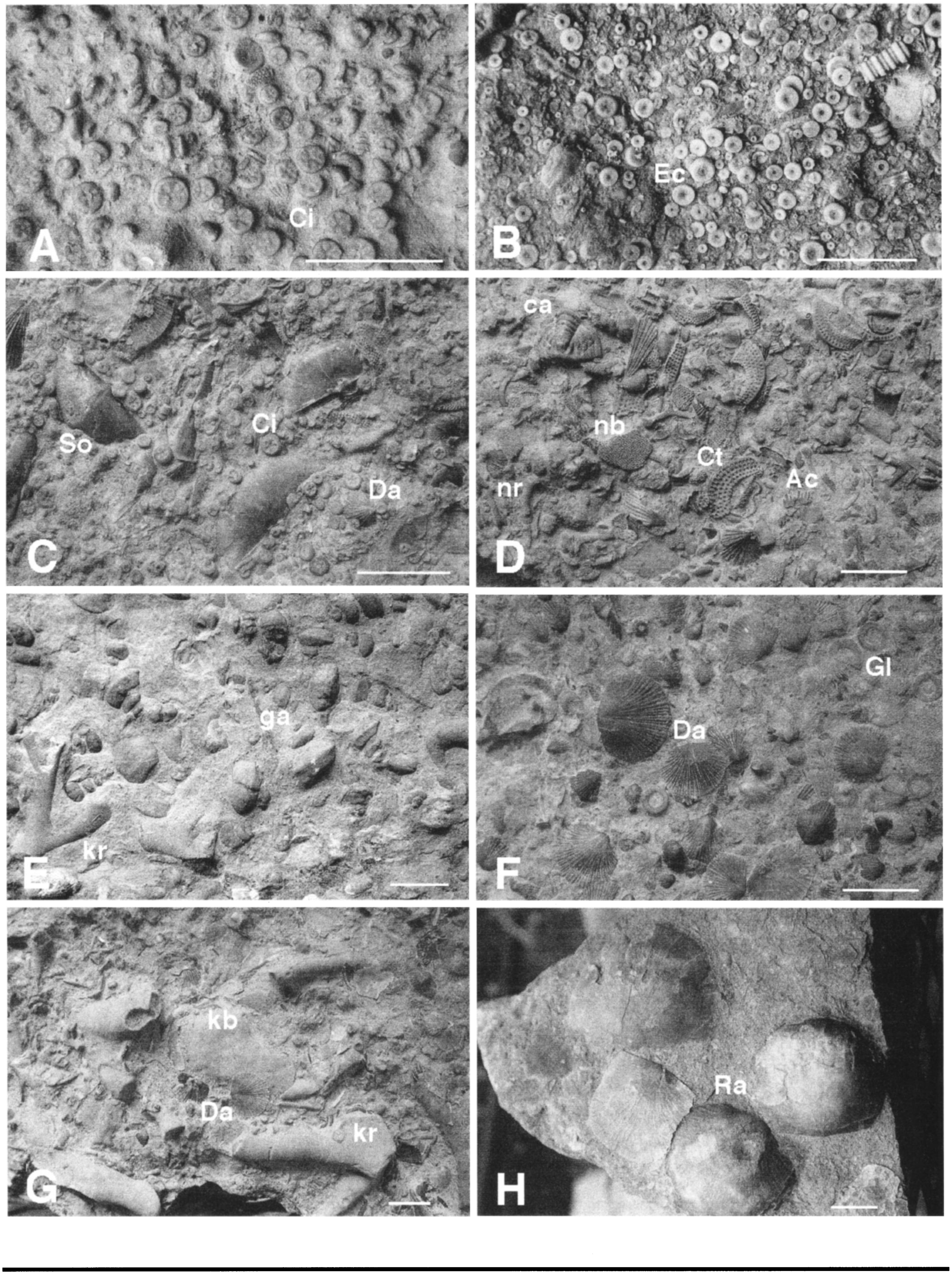
Ci
A
Ec
B
So
Ci
Da
C
ca
nb
Ct
Ac
nr
D
ga
kr
E
Gl
Da
F
kb
Da
kr
G
Ra
H

TABLE 2—Variability around a single axis 1 sample score of 200

Sample #K528.88
C *Dalmanella*
R thick remose bryozoan
R calymenid
R *Isotelus*
R *Ectenocrinus*

Sample #H214.58
C calymenids
C thin ramose bryozoan
R *Sowerbyella*
R *Zygospira*
R *Pseudolingula*
R *Aspidopora*
R thick ramose bryozoan
R *Ambonychia*
R *Acidaspis*
R *Isotelus*
R *Cincinnaticrinus*
R *Ectenocrinus*

Sample #K527.42
C *Isotelus*
R *Dalmanella*
R cephalopod

Sample #B219.56
C *Dalmanella*
R *Sowerbyella*
R *Cyclora*
R thin ramose bryozoan

Sample #K515.24
R *Sowerbyella*
R *Zygospira*
R *Aspidopora*
R thin bifoliate bryozoan
R thick ramose bryozoan
R *Cornulites*
R *Cryptolithus*
R *Iocrinus*

bryozoan, *Rafinesquina*-bryozoan-crinoid, and *Platystrophia*-bryozoan assemblages. Similarly, seriation (Brower and Kile, 1988) has been used previously to reconstruct the principal underlying gradient in Kope assemblages (Holland et al., 2000). The ordering of taxa along DCA axis 1 is correlated highly with that found through seriation (Spearman's r = 0.79, $p<0.001$).

Although these are representative assemblages within the Kope, wide variation in assemblage compositions can be found at a single axis 1 score. For example, when several samples with an axis 1 score of 200 are compared (Table 2), the assemblages have common *Dalmanella* in some cases and none in others, despite having a sample score close to *Dalmanella*'s score of 180. Some of these samples have a diverse bryozoan assemblage whereas others have no bryozoans. This variation at a single axis 1 score may have at least four origins. First, variation is produced in some cases by the origination, extinction, or migration of a taxon in the study area. For example, the crinoid *Merocrinus* is known to occur only in the lowermost Kope. Thus, even at sample scores of 150 (the taxon score for *Merocrinus*) high in the Kope, *Merocrinus* is absent. Second, some compositional variation may result from geographic variation within the study area that is not correlated with water depth. For example, some taxa may be consistently more abundant in some areas than others, for reasons uncorrelated to water depth. Third, differences in assemblage composition may reflect temporal changes in factors not correlated with water depth. Fourth, stochastic variation is almost certainly present in the data. All of these sources of variation may be expressed on axes 2 and 3, although how their effects combine to produce these axes is not obvious.

The variation expressed at a single axis 1 score reflects substantial variation in the composition of assemblages, suggesting that assemblage compositions are not controlled rigidly. To some extent, taxa must have been free to form assemblages of widely varying compositions, an observation at odds with the concept of ecological locking and rigidly defined communities with limited membership (Brett et al., 1996).

Axis 2 appears to reflect differences in life habit and guild membership. Almost all of the taxa with low (<200) axis 2 scores are sessile, low-tier epifaunal suspension feeders. High axis 2 scores reflect taxa with a much wider variety of life habits, including mobile taxa (several of the trilobites, gastropods, cephalopods, ostracods), infaunal taxa (nuculoids, *Modiolopsis,* lingulids), deposit feeders (nuculoids, possibly trilobites and gastropods), carnivores (cephalopods, scolecodonts, hydrozoans), as well as planktic and nektic forms (cephalopods, graptolites). This mollusk-dominated fauna with high axis 2 scores forms a distinctive biofacies (Fig. 4E) that recurs at several horizons throughout the Kope (Brett and Algeo, 1999c).

DCA Axis 1 and Water Depth

As is common in marine ecological data, axis 1 is correlated with water depth, as suggested by several lines of evidence. Several taxa with high axis 1 scores—*Strophomena, Rafinesquina,* and *Platystrophia*—are known to be more abundant in lithofacies shallower than the Kope Formation (e.g., the Fairview Formation, Tobin, 1982; Holland, 1993). These three genera lie at the extreme high end of axis 1, suggesting relatively shallow-water conditions. Because deeper water facies than the Kope are not exposed in Middle and Upper Ordovician rocks from the Cincinnati Arch, it is difficult to make a parallel argument for low values of axis 1. However, several taxa that have relatively low scores, such as *Cryptolithus* and *Sowerbyella,* have been interpreted to be relatively deep-water taxa in the Ordovician of the Appalachian Basin (Bretsky, 1970; Springer and Bambach, 1985). Similarly, the deep-water trilobite *Triarthrus,* too rare to be included in this ordination, also occurred in samples with low axis 1 scores.

As is true for most modern marine invertebrates, depth itself rarely exerts direct control on the distribution of taxa (see review in Holland, 2000). Instead, depth association is governed by physical and chemical factors that have a strong correlation with depth. Based on modern storm-dominated continental shelves, these factors in the Kope likely include frequency of storm disturbance, substrate consistency, temperature, and oxygen levels, although other factors also may have contributed to the observed depth relationship. The type Cincinnatian Series provides clear evidence that storm disturbance decreased into deeper water, as would be expected (Tobin, 1982; Jennette

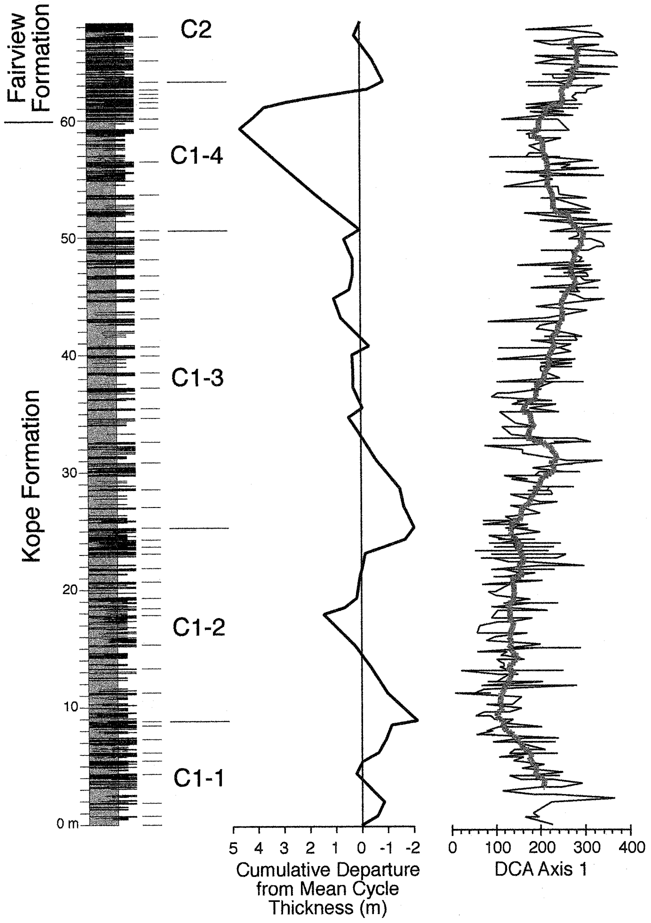

FIGURE 5—K445 section, including sequence stratigraphy, trends in cycle thickness, and axis 1 scores from detrended correspondence analysis. Short lines next to measured section indicate boundaries of meter-scale cycles and numbered 20-m cycles. Central column is a Fischer plot, except that points are placed at meter-scale cycle boundaries, rather than being evenly spaced as in a conventional Fischer plot; this change accentuates the changes in cycle thickness. Deflections to the left indicate a series of thicker-than-average cycles, whereas deflections to the right indicate a series of thinner-than average cycles. Heavy gray line in rightmost column indicates 21-point moving average used to highlight trends; value of 21 was found empirically to balance minimizing local noise while preserving consistent trends.

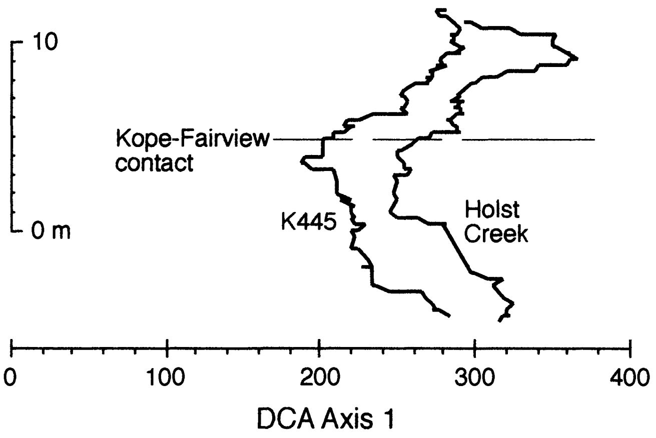

FIGURE 6—Systematic offset of axis 1 scores in depositionally updip Holst Creek outcrop and depositionally downdip K445 outcrop. Note that Holst Creek is consistently offset towards higher values on DCA Axis 1, as would be expected in a shallower water setting.

and Pryor, 1993). The increase in percent mudstone into deeper facies in the Cincinnatian also indicates that substrate consistency was correlated with water depth. When several variables are highly interrelated such that their effects are difficult to tease apart, yet their combined effects can be summarized by a single gradient, they are considered collectively to be a complex gradient (Cisne and Rabe, 1978). In marine settings, depth commonly acts as a complex gradient (Patzkowsky, 1995).

When plotted stratigraphically for the nearly complete Kope section exposed at K445, axis 1 sample scores show a clear overall drift towards higher values above 10 m, with intervals of reversals to lower values (Fig. 5). This overall drift is consistent with previous lithologically based interpretations of the Kope as overall shallowing-upward (Tobin, 1982; Holland, 1993; Jennette and Pryor, 1993) and serves as a third line of evidence that axis 1 correlates with water depth. Furthermore, the Fairview Formation has higher axis 1 values than most of the Kope. This is consistent with the widespread interpretation that the Fairview represents a shallower water facies than the Kope because of the Fairview's lower shale content, greater proportion of proximal storm beds, greater number of grainstone beds, and the greater degree of abrasion, boring, micritization, and encrustation of fossils (Hay, 1981; Tobin, 1982; Holland, 1993; Jennette and Pryor, 1993).

Superimposed on this long-term drift towards higher values are several shifts toward lower values (at 3–9 m, 24–26 m, 31–35 m, 51–59 m). Some of these shifts correspond to an interval of thicker-than-average meter-scale cycles that have been interpreted as reflecting a relative rise in sea level (Jennette and Pryor, 1993; Holland et al., 1997). However, trends in cycle thickness and trends in axis 1 scores generally do not parallel one another. As accommodation changes, it can be manifested by changes in sedimentation rate and rate of water depth change. The two may not necessarily change in concert, a pattern seen here. For example, under increasingly rapid rates of accommodation, deepening may occur while cycles may get thicker or thinner, depending on sedimentation rates. In the case of the Kope, changes in cycle thickness and axis 1 scores both provide information on changes in accommodation.

Finally, when axis 1 scores at K445 are compared to those from the Holst Creek section, K445 scores are systematically lower than Holst Creek scores (Fig. 6). These two sections are hung on the Kope-Fairview contact, a well-defined horizon within a single meter-scale cycle that can be correlated throughout the region. This systematic offset in axis 1 scores confirms that axis 1 correlates with water depth in that the depositionally downdip K445 section has consistently lower values than coeval strata in the depositionally updip Holst Creek section.

Although biofacies analysis normally would proceed with a direct comparison of biofacies to lithology, such a comparison here reveals little in the way of consistent patterns (Fig. 5). For example, the limestone-rich interval from 4–9 m coincides with a drift towards smaller axis 1 scores, whereas the limestone interval from 60–68 m reflects increasing axis 1 scores. Similarly, some limestone-

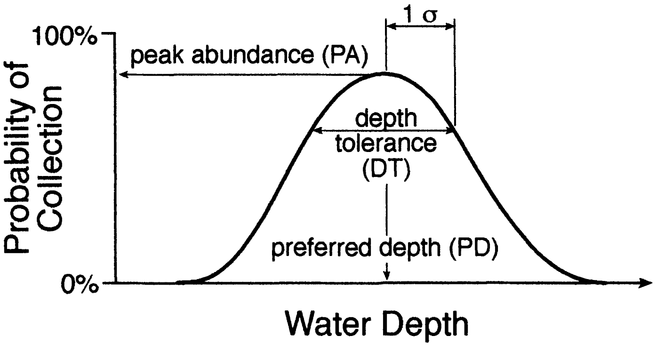

FIGURE 7—Modeling parameters of the distribution of taxa with respect to water depth. Preferred depth is equivalent to the mean of the distribution, depth tolerance is equivalent to the standard deviation, and peak abundance is equivalent to the maximum probability within the distribution.

rich intervals (30–33 m, 48–50 m) correspond to locally high axis 1 values, whereas other limestone-rich intervals (15–19 m, 23–25 m) display no shift in axis 1 values. This lack of correspondence between axis 1 scores and lithological trends also occurs on cross-plots not shown here, which display no linear trends in axis 1 scores with respect to either percent shale or percent limestone. This lack of correspondence suggests that Kope faunas record environmental trends more sensitively than does lithology.

AN ECOLOGICAL MODEL OF THE KOPE

Models of the stratigraphic distribution of fossils have used bell-shaped curves for each taxon that reflect the taxon's probability of occurrence with respect to water depth (Holland, 1995a). Each curve is defined by three parameters (Fig. 7). Preferred depth (PD) is the depth at which the taxon is most abundant or most likely to be found. Depth tolerance (DT) is the standard deviation of the bell-shaped curve and reflects the degree to which the taxon is found in other facies. Peak abundance (PA) is the probability of collecting a taxon at its preferred depth and reflects the overall abundance of a taxon.

These parameters can be estimated from modern taxa, where water depth and abundance of taxa are known from systematic sampling. The shapes of abundance distributions of many types of modern marine taxa suggest that a bell-shaped curve is a reasonable first approximation of the distribution of taxa along ecological gradients; indeed, many ecological models proceed from this approximation (ter Braak and Gremmen, 1987; Holland, in press). Probably the most common departure from this bell-shaped curve seen in modern taxa is a tendency to have an asymmetrical distribution with respect to depth, with a longer tail into deeper water.

Determining these parameters for fossil taxa has not been attempted previously because several obstacles have stood in the way, perhaps the most serious of which was the lack of a quantitative measure of water depth. Because DCA axis 1 scores are correlated with water depth, they solve this problem and can be used as a proxy for water depth within the study interval.

Preferred depth (PD) can be estimated directly from the axis 1 score for each taxon because DCA calculates the taxon score as the abundance-weighted average of sample scores of the samples in which it is found, and vice versa (Hill and Gauch, 1980). Because DCA axis 1 sample and taxon scores are therefore on the same scale, depth tolerance (DT) of a taxon can be calculated as the standard deviation of all axis 1 sample scores in which the taxon occurs. If a taxon occurs in samples arrayed over a wide range along axis 1, its standard deviation will be large, whereas if the taxon occurs only in samples with a narrow range of axis 1 values, its standard deviation will be small. Finally, peak abundance (PA) can be estimated by calculating the percentage of samples in which a taxon occurs within one DT of the PD for the taxon. This percentage is then rescaled to find the true PA, that is, the probability of occurrence at the PD. This rescaling factor is simply the ratio of the PA to the average probability of occurrence within one DT of the PD (see Holland, 1995b for equation describing probability of occurrence). For all but extremely abundant taxa, this scaling factor is 1.186. This approach for estimating PD, DT, and PA is similar to that used in plant ecology for describing the response of plant taxa to environmental parameters (cf. ter Braak and Looman, 1986).

From the values of PD, DT, and PA, a modeled abundance curve can be calculated for each taxon in the Kope (Figs. 8–9; Table 3). Calculated values of PD, given by the axis 1 scores for each taxon, range from −44 to 479 (in axis 1 units, unscaled to depth in meters or other units). Some of these lie outside the observed range of sample scores (0 to 434), indicating that these taxa are most abundant in shallower or deeper conditions than found in the Kope. Actual values of preferred depth may be lower than −44 or higher than 479 for these taxa. Similarly, taxa whose PD is near the edge of the sampled portion of axis 1 also might actually be found to lie farther out on axis 1 with more complete sampling of shallower and deeper water settings.

Values of DT range from 2 to 125, with a mean of 69. After the poorly sampled brachiopod *Schizocrania,* which has a DT of 2, the next lowest value of DT is 46. Thus, of the relatively abundant components of the Kope fauna, DT values vary by a factor of 3. Just as sampling shallower and deeper water environments could cause some values of PD to shift, it also might cause values of DT to increase, particularly for taxa that are eurytopic. Finally, given the length of the sampled gradient in the Kope and the typical DT values, many taxa have some non-zero likelihood of occurrence in much of the Kope, a fact reflected by the widespread view of the Kope as having a single fauna.

PA ranges from 0.3% to 164%, with a mean of 22%. Obviously, the probability of occurrence of a taxon cannot exceed 100%, but calculated values of PA that exceed 100% reflect taxa that are so common that they are guaranteed to be found not only at their PD, but also to some extent in shallower and deeper settings. In the Kope, only the crinoids *Cincinnaticrinus* and *Ectenocrinus* and the ubiquitous brachiopod *Rafinesquina* have PA greater than 100%. Even though observed values of PA in the Kope vary by almost three orders of magnitude, values of PA for all taxa ever reported from the Kope must vary by an even greater amount, because many of these taxa were too rare to be encountered in this study.

Although the Kope was deposited on a storm-dominated ramp, theoretical considerations and field data suggest

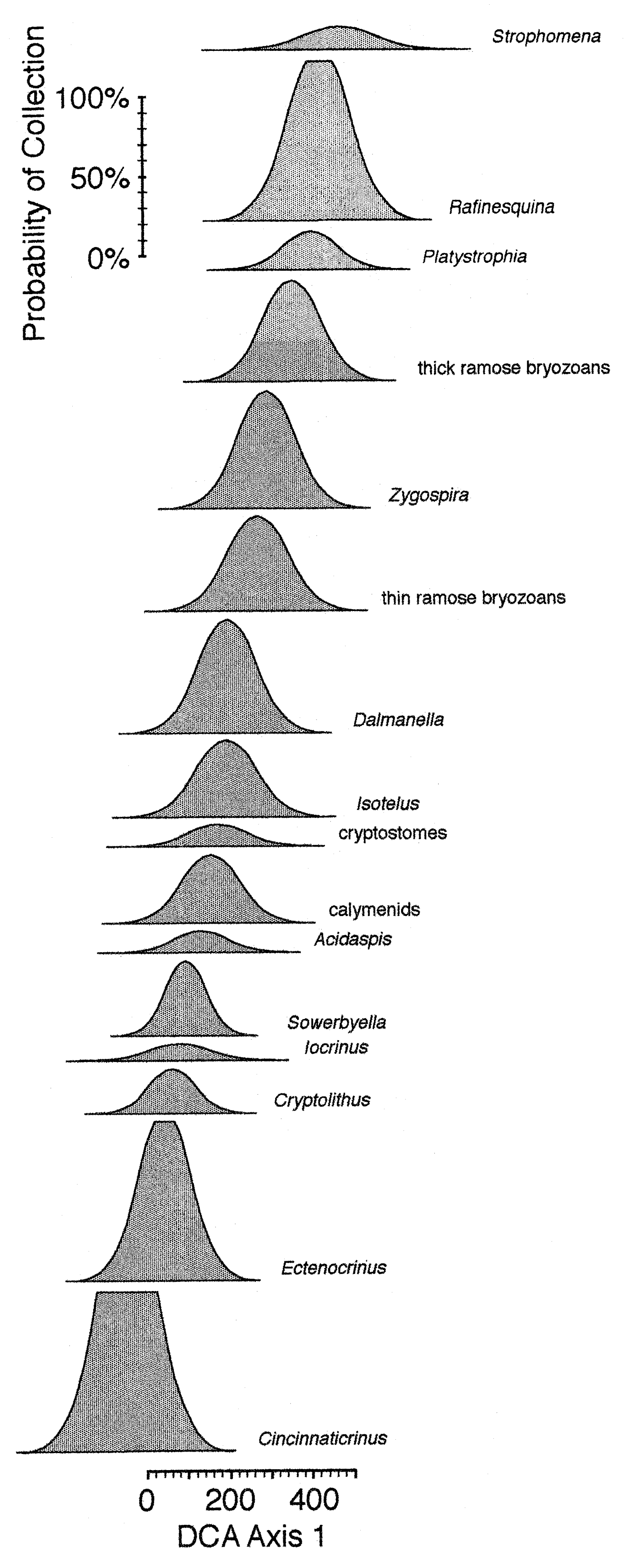

FIGURE 8—Reconstructed ecological distributions of abundant Kope taxa along axis 1. See text for construction of these curves. Note that scale at bottom indicates actual sampled part of gradient; curves beyond these limits are extrapolations and their accuracy is currently unknown.

that post-mortem shell transport is minor. In offshore settings, storm-generated water movement consists of an onshore-offshore wave component that results in little net transport of sediments and an isobath-parallel current component resulting from geostrophic flow that is the principal agent of sediment transport (Duke, 1990). Although Ekman turning of this geostrophic flow causes a slight (~25°) basinward transport of bedload, most larger grains are moved only short distances during storm events (Kachel and Smith, 1986). Furthermore, multiple field studies indicate that out-of-habitat transport is rare in level-bottom sublittoral environments, although many or most individuals undergo some within-habitat transport (Kidwell and Bosence, 1991; Kidwell and Flessa, 1996). Because out-of-habitat shell transport in these settings generally involves small numbers of individuals (Kidwell and Bosence, 1991), transport is more likely to raise values of DT than to cause shifts in PD values. Finally, Miller (1997) found that small-scale faunal patchiness was preserved in the shallower-water and more storm-influenced Fairview Formation and that it could not be explained by post-mortem transport.

DISCUSSION

The most important conclusion to be drawn from this study is that subtle facies control on the distribution of fossils easily can go undetected unless it is sought specifically with analyses designed for that purpose. The Kope has long been treated as a single lithofacies and, as such, its faunas have likewise been viewed simply as variations on an offshore biota. Instead, Kope faunas vary predictably with inferred water depth to a much finer degree than can be detected lithologically. As has been argued elsewhere, benthic faunas can be more sensitive indicators of environmental change than lithofacies (Miller, 1988; Brett, 1998).

Quantified changes in faunal abundance may be used in some cases to infer sequence architecture in a manner similar to coenocorrelation (Cisne and Rabe, 1978). For example, the stratigraphic pattern seen in the moving average of axis 1 sample scores (Fig. 5) matches the textbook well-log pattern of progradational stacking in that it shows a net drift towards shallower values, with well-defined shorter intervals of deepening (i.e., flooding surfaces). Detrended correspondence analysis and other multivariate techniques can supply a single proxy variable for water depth that can be used in this way for sequence stratigraphic interpretations, particularly in monotonous offshore lithofacies such as the Kope. Furthermore, the original data need not consist of actual counts of specimens. The data used here were based on a consistently applied scheme of relative abundance that was later converted to numerical values. Thus, even semiquantitative or rank data can be used to make these interpretations. Similar approaches have been used for single taxa or ratios of taxa (e.g., Sweet, 1979; Armentrout and Clement, 1991), but multivariate approaches have an advantage in that they combine information from all of the taxa into a single metric.

Multivariate approaches also have the advantage of allowing the estimation of three parameters describing fossil distributions: preferred depth, depth tolerance, and

TABLE 3—Calculated values of Preferred Depth, Depth Tolerance, and Peak Abundance.

Taxon	Preferred Depth (PD)	Depth Tolerance (DT)	Peak Abundance (PA)
Acidaspis	138.7	65.9	13.6
Ambonychia	169.9	77.1	3.3
Aspidopora	111.2	46.9	8.8
calymenids	162.2	69.4	42.6
cephalopods	164.5	60.7	1.5
Ceraurus	182.1	59.6	0.4
Cincinnaticrinus	−43.9	71.5	164.2
Cornulites	81.5	70.1	7.6
Craniops	133.1	82.3	1.0
Cryptolithus	68.0	55.7	27.9
cryptostomes	179.6	70.9	13.9
Cyclonema	138.7	80.1	0.3
Cyclora	185.2	56.9	5.1
Dalmanella	204.7	69.1	71.4
Ectenocrinus	48.2	63.3	106.4
encrusting bryozoans	169.2	96.3	2.8
Escharopora	262.1	82.4	3.1
fenestellids	310.7	124.6	0.9
gastropods	133.9	95.3	1.5
Glyptocrinus	94.9	57.4	0.4
graptolites	109.4	57.0	9.8
hydrozoans	369.7	63.4	2.0
Iocrinus	84.7	72.5	10.6
Isotelus	200.5	72.8	48.2
Lepidocoleus	39.2	60.5	5.7
Merocrinus	112.8	61.9	4.8
Modiolopsis	176.6	79.4	0.7
nuculoids	202.3	66.8	1.9
ostracods	138.7	62.6	8.6
Parvohallopora	−19.7	123.8	0.7
Platystrophia	408.9	66.3	24.4
Plectorthis	278.5	101.7	1.0
Prasopora	144.3	49.0	0.5
Proetidella	125.6	49.7	0.6
Pseudolingula	233.2	53.1	1.5
Rafinesquina	430.4	74.5	106.2
Schizocrania	79.6	2.2	*
scolecodonts	285.8	46.1	2.7
Sowerbyella	102.0	48.0	46.9
Stomatopora	−12.3	62.0	4.4
Strophomena	478.8	87.7	14.8
thick bifoliate bryozoans	405.0	70.9	3.7
thick ramose bryozoans	362.5	69.3	63.4
thin bifoliate bryozoans	282.4	76.7	9.7
thin ramose bryozoans	279.0	72.5	59.7
Zygospira	300.7	69.0	73.0

* too few samples to be calculated; poor fit to normal distribution.

peak abundance. The latter two of these parameters provide an additional layer of information in that they allow the facies specificity and abundance of each taxon to be calculated. In particular, although some taxa already were suspected to be more facies controlled than others, estimation of depth tolerance allows this degree of control to be quantified. Similarly, estimation of peak abundance al-

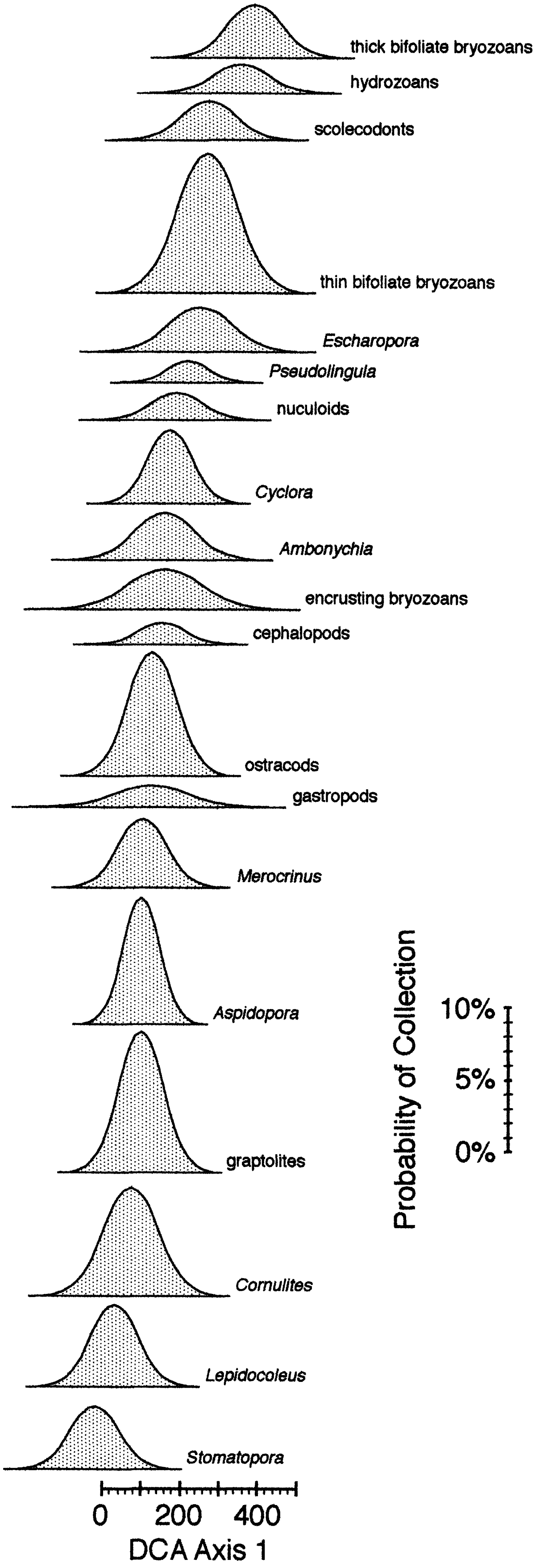

←

FIGURE 9—Reconstructed ecological distributions of rarer Kope taxa along axis 1. See Figure 8 caption for explanation. Note 10x exaggeration in vertical scale relative to Figure 8, necessary because these taxa are much rarer than those in Figure 8.

lows an estimate of the abundance of a taxon that is independent of facies effects.

The ecological model presented here, in which values of PD, PA, and DT are calculated for a range of taxa, has several potential uses. These values could be used to search for long-term stratigraphical, geographical, and macroecological patterns in the distribution, ecological tolerance, and abundance of taxa (cf. Brown, 1984; Brown, 1995). They could be used, in conjunction with axis 1 sample scores, to define fossil recovery potential functions to place confidence limits on fossil ranges, in which the confidence limits would account for changes in facies (Marshall, 1997).

Improved estimates of PD, PA, and DT also can be used to better constrain models of the fossil record (Holland and Patzkowsky, 1999). For example, a conservative estimate of the maximum depth range between the shallowest and deepest facies of the Kope would be 65 m, equivalent to the present compacted thickness of the unit. This can be seen if accommodation was held constant and the Kope simply filled in the available accommodation while not compacting: water depth would decrease by an amount equivalent to the thickness of sediments deposited. However, this simplistic approach neglects the opposing effects of compaction, which would have caused the Kope to have been originally much thicker, and isostatic subsidence, which would diminish the total amount of shallowing during the deposition of the Kope. Backstripping to allow for compaction and isostatic subsidence suggests that the Kope records at most 25–40 m of shallowing. Thus, the depth difference between the highest (434) and lowest (0) axis sample scores would equate to 25–40 m. By this scaling, the average observed value of depth tolerance (69) would equal approximately 4–6 m, over an order of magnitude smaller than that used in Holland and Patzkowsky (1999), suggesting that facies effects on the stratigraphic distribution of fossils are far more severe than previously modeled. Values of PA in this study are also lower than previously modeled, suggesting that phenomena such as the clustering of first and last occurrences at flooding surfaces and sequence boundaries may be masked by the overall rarity of taxa.

The existence of subtle, environmentally controlled variations in the composition of fossil assemblages poses a challenge to biostratigraphic and paleobiologic studies. Facies control itself is already well known. What should now be appreciated is the degree to which it can be developed, how subtly it can be manifested, and how easily it can escape detection. Targeting a single lithofacies in the hope that it will eliminate facies control on fossil distributions may only reduce the magnitude of the problem. Particularly where facies belts are broad and encompass a wide range of water depths, such as offshore and deeper environments, subtle facies control on fossils easily may go undetected. To eliminate this type of facies control, samples should be collected from horizons with similar axis 1 scores, that is, from similar positions along the depth gradient. If this type of subtle facies control is common, it raises the possibility that facies control affects more paleobiologic and biostratigraphic interpretations than currently thought.

CONCLUSIONS

(1) Fossil assemblages within the Kope Formation display subtle environmental control. This control is interpreted to be depth-related because of (A) the known facies distribution of some fossils near the edges of DCA axis 1, (B) the correlation of DCA axis 1 to lithologically-based depth interpretations in vertical section, and (C) systematic differences between DCA axis 1 sample scores from depositionally updip and downdip sections.

(2) A model of depth-related control of Kope faunas is proposed. This model describes the preferred depth, depth tolerance, and peak abundance of the 35 most common taxa examined in this study, principally belonging to the brachiopods, bryozoans, trilobites, mollusks, and echinoderms. Values of depth tolerance appear to be over an order of magnitude smaller than previously modeled, suggesting that facies effects on the stratigraphic distribution of taxa (e.g., clustering of first and last occurrences at flooding surfaces) are more severe than previously modeled.

(3) The detection of facies control where none previously had been documented raises the possibility that facies control can be more subtle than generally accepted. If so, facies effects may exert a much greater influence on some biostratigraphic and paleobiologic patterns than previously thought, particularly in offshore and deeper water facies that are difficult to subdivide based on lithology.

ACKNOWLEDGMENTS

We appreciate the assistance of S. Diekmeyer and T. Reardon in the collection of the field data. We thank T. Algeo and another anonymous PALAIOS reviewer for their reviews of this manuscript. This research was supported by NSF Grants EAR-9204445 to S.M. Holland, and EAR-9204916 to A.I. Miller and D.L. Meyer.

REFERENCES

Anstey, R.L., and Perry, T.G., 1973, Eden Shale bryozoans: A numerical study (Ordovician; Ohio Valley): Michigan State University Paleontological Series, v. 1, p. 1–80.

Anstey, R.L., and Rabbio, S.F., 1990, Regional bryozoan biostratigraphy and taphonomy of the Edenian Stratotype (Kope Formation, Cincinnati Area): Graphic correlation and gradient analysis: PALAIOS, v. 4, p. 574–584.

Anstey, R.L., Rabbio, S.F., and Tuckey, M.E., 1987, Bryozoan bathymetric gradients within a Late Ordovician epeiric sea: Paleoceanography, v. 2, p. 165–176.

Armentrout, J.M., and Clement, J.F., 1991, Biostratigraphic calibration of depositional cycles: a case study in High Island—Galveston—East Breaks areas, offshore Texas: *in* Armentrout, J.M., and Perkins, B.F., eds., Sequence stratigraphy as an exploration tool: Concepts and practices: Gulf Coast Section of SEPM, Houston, p. 21–51.

Bayer, U., and McGhee, G.R., 1985, Evolution in marginal epicontinental basins: The role of phylogenetic and ecologic factors (Ammonite replacements in the German Lower and Middle Jurassic): *in* Bayer, U., and Seilacher, A., eds., Sedimentary and Evolutionary Cycles: Springer-Verlag, New York, p. 164–220.

Bretsky, P.W., 1970, Late Ordovician ecology of the central Appalachians: Peabody Museum of Natural History Bulletin, v. 34, p. 1–150.

Brett, C.E., 1998, Sequence stratigraphy, paleoecology, and evolution: Biotic clues and responses to sea-level fluctuations: PALAIOS, v. 13, p. 241–262.

Brett, C.E., and Algeo, T.J., 1999a, Event beds and small-scale cycles in Edenian to lower Maysvillian strata (Upper Ordovician) of northern Kentucky: identification, origin, and temporal constraints: *in* Algeo, T.J., and Brett, C.E., eds., Sequence, cycle & event stratigraphy of Upper Ordovician & Silurian strata of the Cincinnati Arch region: 1999 Field Conference of the Great Lakes Section of SEPM, Cincinnati, p. 65–92.

Brett, C.E., and Algeo, T.J., 1999b, Sequence stratigraphy of Upper Ordovician and Lower Silurian strata of the Cincinnati Arch region: *in* Algeo, T.J., and Brett, C.E., eds., Sequence, cycle & event stratigraphy of Upper Ordovician & Silurian strata of the Cincinnati Arch region:1999 field conference of the Great Lakes Section of SEPM, Cincinnati, p. 34–46.

Brett, C.E., and Algeo, T.J., 1999c, Stratigraphy of the Upper Ordovician Kope Formation in its type area (northern Kentucky), including a revised nomenclature: *in* Algeo, T.J., and Brett, C.E., eds., Sequence, cycle & event stratigraphy of Upper Ordovician & Silurian strata of the Cincinnati Arch region:1999 Field conference of the Great Lakes Section of SEPM, Cincinnati, p. 47–64.

Brett, C.E., Ivany, L.C., and Schopf, K.M., 1996, Coordinated stasis: An overview: Palaeogeography, Palaeoclimatology, Palaeoecology, v. 127, p. 1–20.

Brower, J.C., and Kile, K.M., 1988, Seriation of an original data matrix as applied to paleoecology: Lethaia, v. 21, p. 79–93.

Brown, J.H., 1984, On the relationship between abundance and distribution of species: The American Naturalist, v. 124, p. 255–279.

Brown, J.H., 1995, Macroecology: University of Chicago Press, Chicago, 269 p.

Caster, K.E., Dalvé, E.A., and Pope, J.K., 1955, Elementary guide to the fossils and strata of the Ordovician in the vicinity of Cincinnati Ohio: Cincinnati Museum of Natural History, 47 p.

Cisne, J.L., and Rabe, B.D., 1978, Coenocorrelation: Gradient analysis of fossil communities and its applications stratigraphy: Lethaia, v. 11, p. 341–364.

Dalvé, E., 1948, The fossil fauna of the Ordovician in the Cincinnati region: University Museum, Department of Geology and Geography, Cincinnati, Ohio, 56 p.

Dattilo, B.F., 1996, A quantitative paleoecological approach to high-resolution cyclic and event stratigraphy: the Upper Ordovician Miamitown Shale in the type Cincinnatian: Lethaia, v. 29, p. 21–37.

Diekmeyer, S.C.S.L., 1998, Kope to Bellevue Formations: the Riedlin Road / Mason Road site (Upper Ordovician, Cincinnati, Ohio region): *in* Davis, R.A., and Cuffey, R.J., eds., Sampling the layer cake that isn't: The stratigraphy and paleontology of the type-Cincinnatian: Ohio Division of Geological Survey Guidebook No. 13, Columbus, p. 10–35.

Duke, W.L., 1990, Geostrophic circulation or shallow marine turbidity currents? The dilemma of paleoflow patterns in storm-influenced prograding shoreline systems: Journal of Sedimentary Petrology, v. 60, p. 870–883.

Harrison, W.B., and Mahan, T.K., 1981, Lower Cincinnatian Kope Formation: *in* Roberts, T.G., ed., GSA Cincinnati '81 field trip guidebooks: American Geological Institute, Falls Church, p. 36–45.

Hay, H.B., 1981, Lithofacies and formations of the Cincinnatian Series (Upper Ordovician), southeastern Indiana and southwestern Ohio: Unpublished Ph.D. Dissertation, Miami University, Oxford, Ohio, 236 p.

Hill, M.O., and Gauch, H.G., Jr., 1980, Detrended correspondence analysis: an improved ordination technique: Vegetatio, v. 42, p. 47–58.

Holland, S.M., 1993, Sequence stratigraphy of a carbonate-clastic ramp: The Cincinnatian Series (Upper Ordovician) in its type area: Geological Society of America Bulletin, v. 105, p. 306–322.

Holland, S.M., 1995a, Depositional sequences, facies control, and the distribution of fossils: *in* Haq, B.U., ed., Sequence stratigraphy and depositional response to eustatic, tectonic and climatic forcing: Kluwer Academic Publishing, Dordrecht, p. 1–23.

Holland, S.M., 1995b, The stratigraphic distribution of fossils: Paleobiology, v. 21, p. 92–109.

Holland, S.M., 2000, The quality of the fossil record—a sequence stratigraphic perspective: *in* Erwin, D.H., and Wing, S.L., eds., Deep time: Paleobiology's perspective: Paleontological Society, Lawrence, p. 148–168.

Holland, S.M., Meyer, D.L., and Miller, A.I., 2000, High-resolution correlation in apparently monotonous rocks: Upper Ordovician Kope Formation, Cincinnati Arch: PALAIOS, v. 15, p. 73–80.

Holland, S.M., Miller, A.I., Dattilo, B.F., Meyer, D.L., and Diekmeyer, S.L., 1997, Cycle anatomy and variability in the storm-dominated type Cincinnatian (Upper Ordovician): Coming to grips with cycle delineation and genesis: Journal of Geology, v. 105, p. 135–152.

Holland, S.M., Miller, A.I., and Meyer, D.L., 1999, Sequence stratigraphy of the Kope-Fairview interval (Upper Ordovician, Cincinnati, Ohio area): *in* Algeo, T.J., and Brett, C.E., eds., Sequence, cycle & event stratigraphy of Upper Ordovician & Silurian strata of the Cincinnati Arch region: 1999 field conference of the Great Lakes Section of SEPM, Cincinnati, p. 93–102.

Holland, S.M., and Patzkowsky, M.E., 1999, Models for simulating the fossil record: Geology, v. 27, p. 491–494.

Jennette, D.C., and Pryor, W.A., 1993, Cyclic alternation of proximal and distal storm facies: Kope and Fairview Formations (Upper Ordovician), Ohio and Kentucky: Journal of Sedimentary Petrology, v. 63, p. 183–203.

Kachel, N.B., and Smith, J.D., 1986, Geological impact of sediment transporting events on the Washington continental shelf: *in* Knight, R.J., and McLean, J.R., eds., Shelf sands and sandstones: Canadian Society of Petroleum Geology, p. 145–162.

Kenkel, N.C., and Orlóci, L., 1986, Applying metric and nonmetric multidimensional scaling to ecological studies: Some new results: Ecology, v. 67, p. 919–928.

Kidwell, S.M., and Bosence, D.W.J., 1991, Taphonomy and time-averaging of marine shelly faunas: *in* Allison, P.A., and Briggs, D.E.G., eds., Taphonomy: Releasing the Data Locked in the Fossil Record: Plenum Press, New York, p. 115–209.

Kidwell, S.M., and Flessa, K.W., 1996, The quality of the fossil record: Populations, species, and communities: Annual Review of Earth and Planetary Sciences, v. 24, p. 433–464.

Kreisa, R.D., Dorobek, S.L., Accorti, P.J., and Ginger, E.P., 1981, Recognition of storm-generated deposits in the Cincinnatian Series, Ohio: Geological Society of America Abstracts with Programs, v. 13, p. 285.

Lorenz, D.M., 1973, Edenian (Upper Ordovician) benthic community ecology in north-central Kentucky: Dissertation Abstracts International, v. 34B, p. 2816.

Marshall, C.R., 1997, Confidence intervals on stratigraphic ranges with nonrandom distributions of fossil horizons: Paleobiology, v. 23, p. 165–173.

McCune, B., and Mefford, M.J., 1997, PC-ORD. Multivariate Analysis of Ecological Data, Version 3.0: Gleneden Beach, Oregon, MjM Software Design.

Miller, A.I., 1988, Spatial resolution in subfossil molluscan remains: Implications for paleobiological analyses: Paleobiology, v. 14, p. 91–103.

Miller, A.I., 1997, Counting fossils in a Cincinnatian storm bed: spatial resolution in the fossil record: *in* Brett, C.E., and Baird, G.C., eds., Paleontological events: Stratigraphic, ecological, and evolutionary implications: Columbia University Press, New York, p. 57–72.

Miller, A.I., Holland, S.M., Dattilo, B.F., and Meyer, D.L., 1997, Stratigraphic resolution and perceptions of cycle architecture: Variations in meter-scale cyclicity in the type Cincinnatian Series: Journal of Geology, v. 105, p. 737–743.

Minchin, P.R., 1987, An evaluation of the relative robustness of techniques for ecological ordination: Vegetatio, v. 69, p. 89–107.

Patzkowsky, M.E., 1995, Gradient analysis of Middle Ordovician brachiopod biofacies: Biostratigraphic, biogeographic, and macroevolutionary implications: PALAIOS, v. 10, p. 154–179.

Sheldon, P.R., 1996, Plus Áa change—a model for stasis and evolution in different environments: Palaeogeography, Palaeoclimatology, Palaeoecology, v. 127, p. 209–228.

Springer, D.A., and Bambach, R.K., 1985, Gradient versus cluster analysis of fossil assemblages: A comparison from the Ordovician of southwestern Virginia: Lethaia, v. 18, p. 181–198.

Sweet, W.C., 1979, Conodonts and conodont biostratigraphy of post-

Tyrone Ordovician rocks of the Cincinnati region: United States Geological Survey Professional Paper, v. 1066-G, p. 1–26.

ter Braak, C.J.F., and Gremmen, N.J.M., 1987, Ecological amplitudes of plant species and the internal consistency of Ellenberg's indicator values for moisture: Vegetatio, v. 69, p. 79–87.

ter Braak, C.J.F., and Looman, C.W.M., 1986, Weighted averaging, logistic regression and the Gaussian response model: Vegetatio, v. 65, p. 3–11.

Tobin, R.C., 1982, A model for cyclic deposition in the Cincinnatian Series of southwestern Ohio, northern Kentucky and southeastern Indiana: Unpublished Ph.D. Dissertation, University of Cincinnati, 483 p.

Tobin, R.C., 1986, An assessment of the lithostratigraphic and interpretive value of the traditional "biostratigraphy" of the type Upper Ordovician of North America: American Journal of Science, v. 286, p. 673–701.

Weir, G.W., Peterson, W.L., Swadley, W.C., and Pojeta, J., 1984, Lithostratigraphy of Upper Ordovician strata exposed in Kentucky: United States Geological Survey Professional Paper, v. 1151-E, p. 1–121.

Weiss, M.P., and Sweet, W.C., 1964, Kope Formation (Upper Ordovician)—Ohio and Kentucky: Science, v. 145, p. 1296, 1301–1302.

Wilson, M.A., 1985, Disturbance and ecologic succession in an Upper Ordovician cobble-dwelling hardground fauna: Science, v. 228, p. 575–577.

ACCEPTED DECEMBER 14, 2000

APPENDIX: LOCALITY DESCRIPTIONS

Hume: Roadcut along west side of US Route 42, 0.3 mile north of intersection with Kentucky State Route 14 at town of Hume near intersection with Kentucky State Route 338, just south of Beaverlick, Kentucky. Verona, KY 7 1/2′ quadrangle. 38° 50′ 48″ N, 84° 43′ 00″ W.

Holst Creek: Series of roadcuts on northeast side of AA Highway (Kentucky State Route 9) at intersection with Kentucky State Route 1019 and proceeding downhill to the northwest for 0.6 miles to intersection with Holst Creek Road, south of Foster, Kentucky. Moscow, OH-KY 7 1/2′ quadrangle. 38° 46′ 33″ N, 84° 12′ 20″ W.

K445 Composite. Composite outcrop consists of four sections: K445, CON1, CON2, and CON3. K445: Roadcut on both sides of Kentucky State Route 445, 0.2 km west of intersection with Kentucky State Route 8, immediately northwest of the I-275 bridge over the Ohio River near Old Coney Amusement Park. Newport, KY-OH 7 1/2′ quandrangle. 39° 03′ 22″ N, 84° 26′ 10″ W. CON1: First roadcut on northwest side of westbound I-275, 0.5 km southwest of intersection of I-275 and the Kentucky bank of Ohio River near Old Coney Amusement Park. Newport, KY-OH 7 1/2′ quadrangle. 39° 03′ 15″ N, 84° 26′ 20″ W. CON2: Second roadcut on northwest side of westbound I-275, 0.6 km southwest of intersection of I-275 and the Kentucky bank of Ohio River near Old Coney Amusement Park. Newport, KY-OH 7 1/2′ quadrangle. 39° 03′ 13″ N, 84° 26′ 24″ W. CON3: Third roadcut on northwest side of westbound I-275, 0.8 km southwest of intersection of I-275 and the Kentucky bank of Ohio River near Old Coney Amusement Park. Newport, KY-OH 7 1/2′ quadrangle. 39° 03′ 10″ N, 84° 26′ 30″ W.

Aurora: Hillside exposure behind the River Creek Village shopping plaza at intersection of Wilson Creek Road and US Route 50, 2.3 miles south of intersection of US Route 50 and Indiana Route 48 at the bridge over Tanners Creek. Aurora, IN-KY 7 1/2′ quadrangle. 39° 04′ 37″ N, 84° 53′ 45″ W.

Miamitown: Composite of two sections. (1) Roadcut along south and north sides of eastbound off-ramp from I-74 at exit #7 for Ohio State Route 128, south of Miamitown, Ohio. Addyston, OH-KY 7 1/2′ quadrangle. 39° 12′ 21″ N, 84° 42′ 34″ W. (2) Roadcut along north side of westbound I-74, at end of onramp at exit for #7 for Ohio State Route 128. Addyston, OH-KY 7 1/2′ quadrangle. 39° 12′ 28″ N, 84° 42′ 43″ W.